Intl. J. Humanities (2013) Vol. 20 (2): (79-100)

Snow Runoff Modeling Using Meteorological, Geological and Remotely Sensed Data

Nastaran Saberi[1], Saeid Homayouni[2], Mahdi Motagh[3]

Received: 2012/3/5 Accepted: 2013/1/1

Abstract

Geographic information and analysis provide a wide range of data and techniques to monitor and manage natural resources. As an important case, in arid and semi-arid areas, water management is critical for both local governance and citizens. As a result, the estimation of potential water brought by snowmelt runoff and rainfalls has a significant importance for these dry areas. Hydrological modeling needs vast knowledge about integrating all relating parameters. In this work, different data sources including remote sensing observations and meteorological and geological data are integrated to supply spatially detailed inputs for snowmelt runoff modeling in a watershed located in Simin-Dasht basin in the northeast of Tehran, Iran. Because of high temporal frequency and suitable spatial coverage, MODIS products have been chosen to derive snow cover area. The MODIS 8-day snow map product with an spatial resolution of 500m (MOD10A2.5) is used. In addition, during the snowmelt period in 2006-2007, archived meteorological and geological data are used to provide parameters and variables for empirical Snow Runoff Modeling (SRM). Landsat ETM+ images with a higher spatial resolution of 30m and less temporal coverage of 16 days are used in 2007 snowmelt period to compare the model accuracy using snow cover area estimations from different sources. Evaluation of the runoff outputs in both models, using in situ measurements, reveals good agreements that prove SRM capability in modeling basin's daily and weekly runoff. Model accuracy shows better satisfactory of snow runoff modeling results that employ Snow Cover Area (SCA) derived from

1 PhD student, RS, Department of Geography, University of Waterloo, nsaberi@uwaterloo.ca
2 Assistant Professor, Department of Geography, University of Ottawa, homayounis@ut.ac.ir
3 Assistant Professor, Department of Geomatics, University of Tehran, motagh@ut.ac.ir

Landsat ETM+ data compared to MODIS snow product modeling. Although, using MODIS SCA the model accuracy was less, still due to less further process and providing better temporal coverage during snowfall and snowmelt season MODIS is recommended. Future works in this criterion could be concentrated on SRM forecast improvement using data assimilation techniques or coupling the empirical model to physical models.

Keywords: Snowmelt Runoff Modeling; MODIS; Landsat ETM+; Snow Cover Area; Meteorological Data.

1. Introduction

Forecasts related to water cycle are highly affected by seasonal snow cover. Melted water from a snowpack or ice layer reserve soil humidity in mountainous catchments and this will be continued till the end of melting season (DeWalle and Rango, 2008). Using remote sensing observations in monitoring snow cover area and thus modeling snowmelt runoff is an efficient monitoring technique that is attributed to the high spatial and temporal variability of snow cover (Nagler, Rott *et al.*, 2008). In addition, gathering *in-situ* measurements of snow physical properties in high spatial and temporal details and over big basins is not a feasible way for providing suitable required data for modeling (Liang, 2008).

Many models have been used to calculate and forecast snow runoff. Models for snow properties and runoff retrieval are divided into empirical and physical approaches. Physical models are more sophisticated and can be used for different areas without critical changes and calibration needed. The only drawback is their requirements; these models have many parameters and variables, which make them not quite applicable in some cases. One example of physical models that has been widely used is the energy balance model. The second group is empirical models in which empirical formulas and relations are used to model the runoff amount. In comparison with physical models, empirical models require less parameters and variables, so applying these models is faster and easier. A disadvantage of empirical models is requiring calibration for different study areas, which then results "home made" versions.

In this paper, an empirical snowmelt runoff modeling, SRM[1] developed by Martinec (Martinec, Rango et al., 1998) has been employed. Due to high temporal frequency and suitable spatial coverage of MODIS optical images, MODIS 8-day snow map product with spatial resolution of 500m (MOD10A2.5), has been chosen to map snow cover. Archived meteorological and geological data are used to provide SRM parameters and variables. Landsat ETM+ images with better spatial resolution (30m) and less temporal coverage (16 days) are also used to compare the model accuracy in same conditions. A review on snow mapping via remote sensing techniques and study area description are brought in sections 2 and 3 respectively. Then implied methodology as well as results and conclusion have been discussed in sections 4, 5, and 6, respectively.

2. Literature Review

Hitherto, the Runoff Model (SRM) by Martinec (Martinec, Rango et al., 1998) is the only widely empirical applied model optimized for remotely sensed snow cover data as an input variable (Najafzadeh, Abrishamchi et al., 2004). In this model, the snowmelt is calculated using the SCA derived from remotely sensed images with respect to degree-days. Most of the other models, such as physical models, need estimation of various parameters and measuring many variables to calculate the net energy that melts the snowpack.

Due to large possibilities of exploiting widely different parts of the electromagnetic spectrum to learn more about the snowpack resource, monitoring snow surface and its hydrological properties can be performed using various satellite images. In the visible spectrum, fraction of the basin covered by snow could be mapped because of the difference in reflectance of snow and snow-free areas. The near infrared portion can also be used for snow mapping and for the detection of near surface liquid water. In the microwave portion, the snowpack emission and attenuation depend on the size and shape of crystals and the presence of liquid water (DeWalle and Rango, 2008).

Snow detection based on optical images was the first step in this application. It has been done through visual interpretation and manual digitizing on Landsat Multi Spectral

1 Snowmelt Runoff Model

Scanner Images (Rango, 1980). Around ten years afterwards, snow cover digital mapping procedure has been replaced with the manual digitizing (Baumgartner and Apfl ,1994; Michael and Baumgartner, 1995). To improve the SCA accuracy, fractional snow cover algorithms are applied to estimate SCA in sub pixel resolution (Dadashi khanghah and Matkan, 2007; Dobreva and Klein, 2011).

Thermal infrared remote sensing has minor potential for snow mapping and snow hydrology. On the other hand, passive microwave radiometry have been used widely to estimate the snow properties such as Snow Water Equivalent (SWE) (Vuyovich and Jacobs, 2011). Moreover, active microwave sensors, especially Synthetic Aperture Radar (SAR) have been also used widely to estimate snow properties. In addition the microwave imagery can help to discriminate easily the snow from other surfaces (Elachi and Van Zyl, 2006; Liang, 2008).

In recent years, fusion methods have been utilized in multi-sensor approaches for monitoring SCA and Snow Surface Wetness (SSW). This has been resulted in developing data assimilation techniques to operationally forecast the runoff in short-term by satellite-based remote sensing techniques (Solberg, Koren *et al*., 2010).

3. Study Area

The Firuzkuh area, (34 N, 51 E) is a 1576Km^2 catchment to the Hablerud River in south of Alborz Mountains and North-East of Tehran, Iran. This basin altitude ranges from 980 to 4036 m. This basin is chosen for snow runoff modeling with respect to high amount of snow cover area during cold season and consequently high amount of melted water in spring. Figure 1 shows the location of this basin.

Figure 1. Study area location

4. Methodology

4.1. Datasets

Using SRM, required parameters and variables should be supplied. These requirements include satellite data, *in-situ* measurements and ancillary maps. Datasets used in this study that have been categorized in three groups, are described in Figure 2.

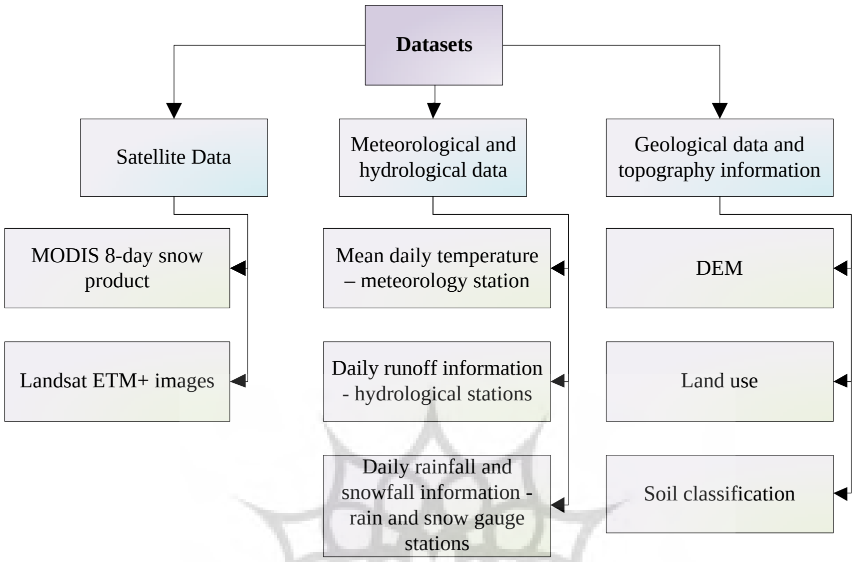

Figure 2. Various datasets used for the snow runoff modeling

4.2. Pre-Process

Pre-process contain several steps to derive model requirements. The information includes parameters and variables required to model snowmelt runoff. Figure 3 shows pre-process steps for the three datasets mentioned in the dataset section. Aforementioned steps are described in subsections 3.2.1 to 3.2.3.

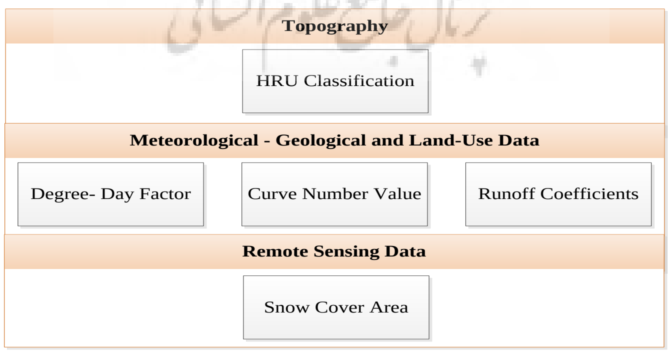

Figure 3. Pre-process steps to derive model input requirements

4.2.1. Topography

The altitude of the basin ranges from 980 to 4036 meters and 6 sub-basins zones or HRU (Hydrological Response unit) are derived as shown in Figure 4. The mean hypsometric elevation of the zone (which is also called mean elevation for ease of use) determined by an area-elevation curve using the Digital Terrain Model (DTM) of the basin with balancing the area below and above the mean elevation. ASTER[1] DTM data with spatial resolution of 30 meters has been used after a Fill Sink correction pre-process in ArcGIS software.

1The Advanced Space borne Thermal Emission and Reflection Radiometer

Table 1 Sub-basin representa

Table 1 explains characteristics of zones. Regarding mean hypsometric elevation calculation, representative stations of defined elevations are positioned with respect to meteorological stations positioning to obtain a good spatial distribution in the area. Figure 4 shows stations with mean hypsometric elevation for the sub-basin that will be used to represent the sub-basin state (a mean value of variables and parameters after interpolation, such as precipitation, runoff coefficients, snow cover area.).

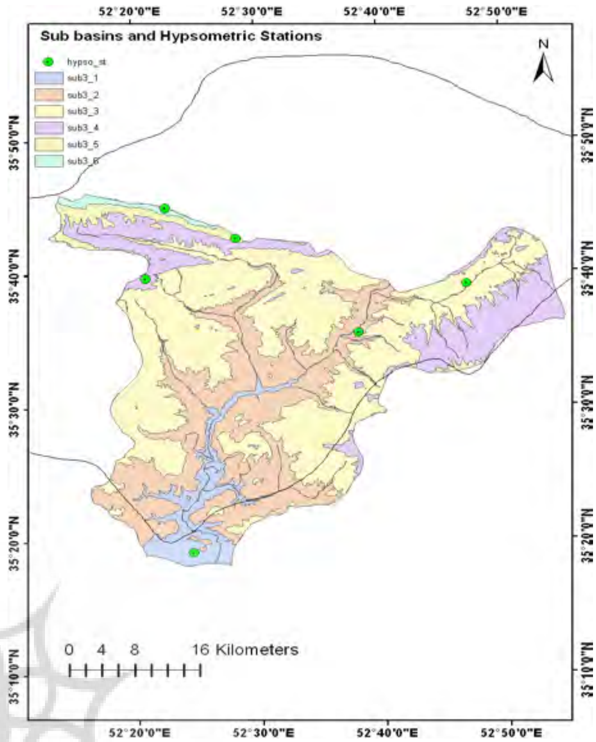

Figure 4. Sub-basin zones and representatives

Table 1 Sub-basin representatives characteristics

Sub-basins Zones Elevation Range	$\frac{Sub-basin\ Area}{Basin\ Area}$ %	Mean Hypsometric Elevation
Sub-basin 1 (950-1500 m)	6.8596	1323.58
Sub-basin 2 (1500-2000 m)	28.0847	1779.37
Sub-basin 3 (2000-2500 m)	46.2237	2226.66
Sub-basin 4 (2500-3000 m)	15.0407	2704.47
Sub-basin 5 (3000-3500 m)	2.7551	3179.90
Sub-basin 6 (3500-4036 m)	1.0343	3694.74

4.2.2. Meteorological and Geological Data

Meteorological data includes daily rainfall and runoff, mean daily temperature and snow properties. This dataset has been collected from synoptic and climatologic stations as wells as *in-situ* measurements. TIN[1] interpolation was applied on meteorological data to derive daily variables for the whole basin. Best station selection to enter interpolation process was done using 2 and 5 kilometers buffer analysis (nearest stations), stations in a 5 kilometer buffer were added only if they had similar geological data (soil hydrologic group and land-use), while compared to the mean elevation representative station.

The geological data is then used to classify the hydrologic soil group (A-to-D) with respect to tables given by Cronshey *et al.,* (1986) for the classification of different materials in soil groups and for Curve Number (*CN*) calculation considering the land-use data. The *CN* is an index for computation of basin's Lag Time (T_{lag}), potential maximum soil moisture retention and runoff coefficients (Cronshey *et al.*, 1986). In this research, we used *CN* relations with runoff coefficients; applied empirical formulas are included at the end of this section. However there are different methods that are more sophisticated for runoff coefficients derivations compared to the method that is used here, but these models need more variables to be measured.

The soil *CN* values, for every of 50 by 50 meter pixel, are computed by rasterizing hydrologic soil group and different land-use classes maps. Result's cell values contain, *Soil Hydrologic group + Land-use class *10,* which could be transformed to curve number value using a look-up table of curve numbers for each land-use class and corresponding soil hydrologic group (Cronshey *et al.*, 1986). Using *CN* raster map, average values are computed for each sub-basin. Hydrologic soil group and different land cover/use classes in the region are shown in Figure 5 and Figure 6.

1. Triangulated Irregular Network

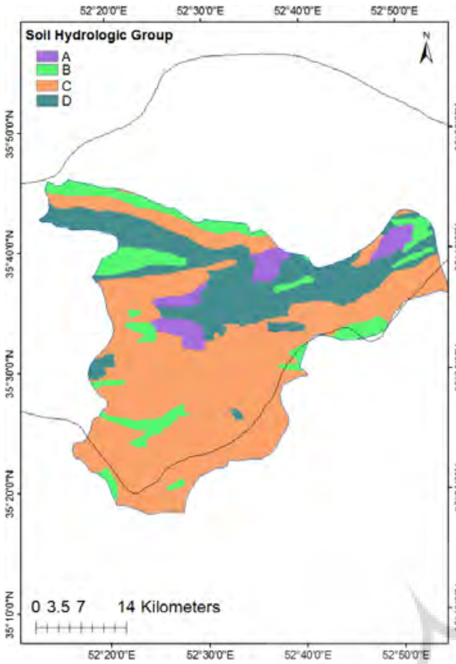

Figure 5. Soil hydrologic group

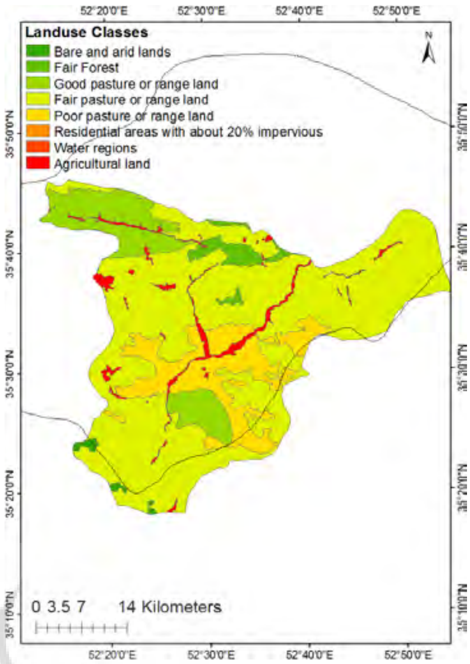

Figure 6. Land-use class

CN can be used to calculate *S*-potential maximum soil moisture retention (in inches) by equation (1).

$$s = \frac{1000}{CN} - 10 \qquad \textbf{(1)}$$

Then lag time is estimated by equation (2), which is the time difference between the start of increasing temperatures and the corresponding increase in runoff from the basin (Martinec, Rango, and Roberts, 1994). Lag time is mainly determined from the hydrographs of the past years, but lack of this knowledge leads us to apply empirical formula developed by Soil Conservation Service (SCS) of United States (Cronshey *et al.*, 1986).

$$T_{lag} = \frac{L^{0.8}(S+1)^{0.7}}{1900y^{0.5}} \qquad \textbf{(2)}$$

In this formula, *L* is the maximum river length of the basin (in feet) and *y* is the average slope of basin (%). T_{lag} will be obtained in an hourly unit and should be rounded by the nearest integer value. In equations (3) to (6), examples of T_{lag} usage in the SRM have been brought (Martinec *et al.*, 1994). It shows contributions of input on the nth day (I_n) and n+1th (I_{n+1}) day with different lag times, which results in Q_{n+1}/ Q_{n+2} day's runoff after being processed by the SRM. In our study area T_{lag} was estimated 5.6, so equation (3) used for SRM process.

T_{lag} =6h , 0.50.I_n +0.50.In+1→ Qn+1 **(3)**

T_{lag} =12h , 0.75.I_n +0.25.I_n+1 → Q_{n+1} **(4)**

T_{lag} =18h , I_n→ Q_{n+1} **(5)**

T_{lag} =24h , 0.25.I_n +0.75.I_n+1→ Q_{n+2} **(6)**

Runoff coefficients (rainfall and snow) are then computed by the equation (7), resulted from fraction of runoff height to precipitation height (*P* is precipitation height in inches) and runoff height is derived by the equation (8).

$$C = \frac{R}{P} \quad \textbf{(7)}$$

$$R = \frac{(P-0.2S)^2}{(P+0.8S)} \quad \textbf{(8)}$$

4.2.3. Optical Remotely Sensed Images

For this study, the MODIS's 8-day product, with a 500m spatial resolution, is used to determine the SCA. This product has the lowest percent of cloud coverage, due to monitoring of maximum snow extent during eight consecutive days. Landsat ETM+ images with a higher spatial resolution and a lower temporal resolution are also used to compare the results of models with different inputs of SCA.

4.2.3.1. MODIS Snow Product

The Moderate Resolution Imaging Spectro-radiometer (MODIS) snow products are provided in a swath and tile format and different spatial and temporal transformation, e.g., 8-day 500 meters spatial resolution product (Zhang, 2004; Riggs, Hall *et al.*, 2007). The MOD10A2.5 product is available in global coverage and 8-day composite that has less cloud pixels in maximum 8-day snow-extent dataset and could lead to a more accurate snow cover map. The pixel values that depict the maximum of snow cover are used due to an unstable climate condition in the mountainous regions (Riggs and Hall, 2011).

To obtain the best estimation, the snow product has been ignored in the condition that cloud cover percentage in the basin is more than 10% of the basin. The SCA is then interpolated using the linear method to obtain the daily snow cover in the condition that the temperature is lower than snowmelt critical degree (*Tc*). For higher temperature degrees, SCA is calculated using equations (9) and (10). Where, ΔM is volume of melted water between t_1 and t_2, a is degree-day factor and T^+ is a counter for degrees higher than *Tc*.

$$\Delta M(t_1,t_2)=\sum_{t_1}^{t_2} aT^+ \tag{9}$$

$$SCA(t_x)=SCA(t_{x-1})-\frac{SCA(t_1)-SCA(t_2)}{\Delta M(t_1,t_A)+\Delta M(t_E,t_2)}\Delta M(t_{x-1},t_x) \tag{10}$$

a, degree-day factor, indicates the snowmelt depth resulting from one degree-day and is obtained by an empirical equation:

$$a=1.1\frac{\rho_s}{\rho_w} \tag{11}$$

where, ρ_s is the snow density and ρ_w is the water density. Using *in-situ* measurements degree-day factor calculated for specific dates and interpolated for snow season during each ten days period. *Tc*, snowmelt critical degree is a discriminator of measured or forecasted precipitation type (rain/snow). Due to lack of comprehensive information, *Tc* has been determined in a range of 0 to 3° c with respect to basin climate and last studies done (Martinec *et al*., 1994).

Figure 7 shows SCA percentage in the sub basins during 2006-2007 periods. Snow depletion curve correction, with respect to degree-day factor and daily temperature above the critical temperature in melting season is applied. Depletions curves in the six HRUs are shown in Figure 8.

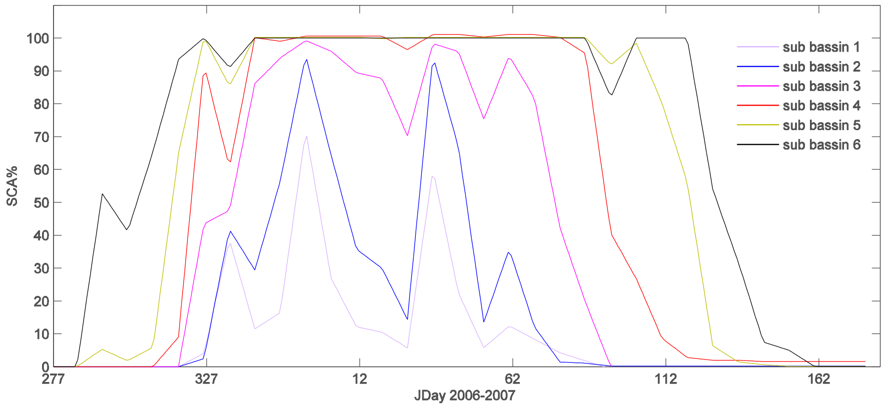

Figure 7. SCA derived by MOD10A2 during 2006-2007

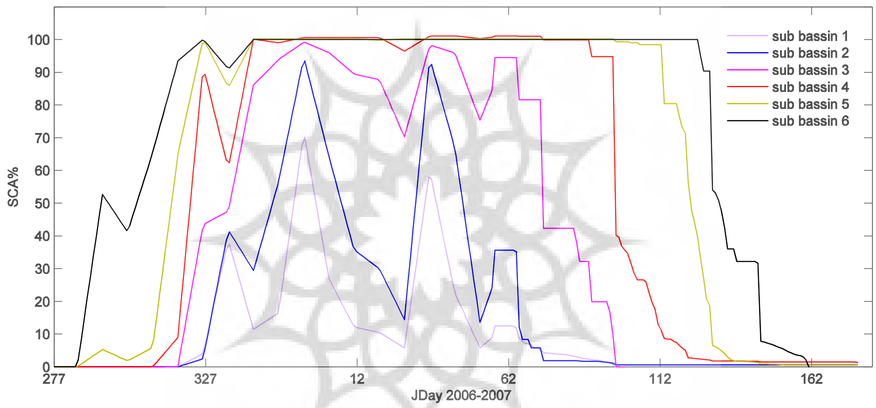

Figure 8. Corrected SCA derived by MOD10A2 during 2006-2007

4.2.3.2Landsat ETM+ 7

The Enhanced Thematic Mapper Plus (ETM+) is an onboard sensor of Landsat 7 satellite with approximate revisit time of 16 days (Irish, 2000). Landsat ETM+ acquires data in eight spectral bands. Four of the eight spectral bands are mostly used in snow classification algorithms.

- Band-2 (B2): 0.53 to 0.61 µm, Green, 30 m resolution
- Band-4 (B4): 0.78 to 0.90 µm, Near Infrared, 30 m resolution
- Band-5 (B5): 1.55 to 1.75 µm, Shortwave Infrared, 30 m resolution
- Band-6 (B6): 10.4 to 12.5 µm, Thermal Infrared, 60 m resolution.

In the methodology developed by Irish, Barker *et al.* (2006) band-6 in low gain after conversion to at-satellite apparent brightness temperature is used. Using different regions of interest from clouds and snow pixels, we found that cloud and snow temperature are close together and even overlap in some areas. Consequently, the 6^{th} band information was not used in the classification algorithm. Level 1 Geometrically corrected product has been used to obtain SCA from each image. It should be noted that from 2003, ETM+ Scan Line Corrector (SLC) has been out of order and as a result all captured images have gaps. Applied processes are shown in Figure 9.

As a result of similar optical properties in cloud and snow pixels, procedure starts with images that have less than 20% percent of cloud cover.

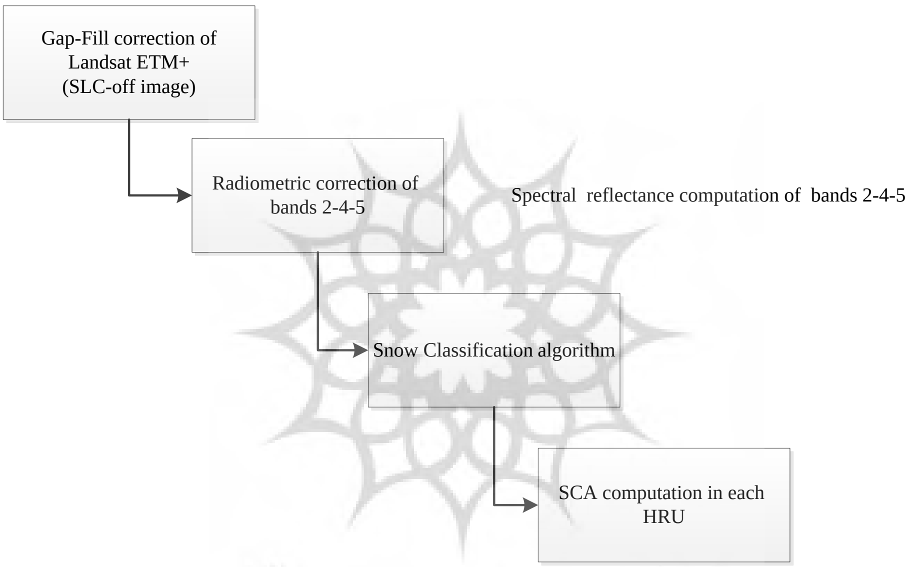

Figure 9. Landsat ETM+ snow classification algorithme

For filling data gaps, an alternative interpolation method, the kriging geostatistical technique, was used (this is applied using ENVI software ETM+ Filling Gap add-on tools) (Zhang, Li *et al.* 2007). After the gap-filling, the radiometric correction has been applied using the specific calibration parameters derived from Chander *et al.*'s (2009) work (Chander, Markham *et al*., 2009). Then the spectral reflectance in bands 2 and 5 are used to calculate the NDSI (Normalized Difference Snow Index). The snow classification implemented by Hall, Riggs *et al*., (2001), snow discrimination algorithm, was applied on MODIS images. Hall algorithm is conformed to Landsat bands using the equation 12. The output class labels is 0 for no snow and 1 for snow class.

$$Snow = NDSI > 0.4 \& b4 > 011 \& b2 > 0.1 \quad \textbf{(12)}$$

Moreover, snow detection based on the Automatic Cloud Cover Assessment Algorithm (ACCA) algorithm is applied using:

$$Snow = NDSI > 0.7 . \quad \textbf{(13)}$$

The classification's overall accuracy in the scene, with 60% percent of cloud cover, was 95.6% and 87.8% with first and second method as described above (equations (3) and (4)). To estimate the accuracy, snow pixels are collected with respect to interpolated temperature and specific visual pattern of snow. Due to the better results of conformed Hall snow classification; this method is applied on all images obtained during 2006-2007. Figure 10 shows results of both algorithms for Landsat image of 2006/10/23.

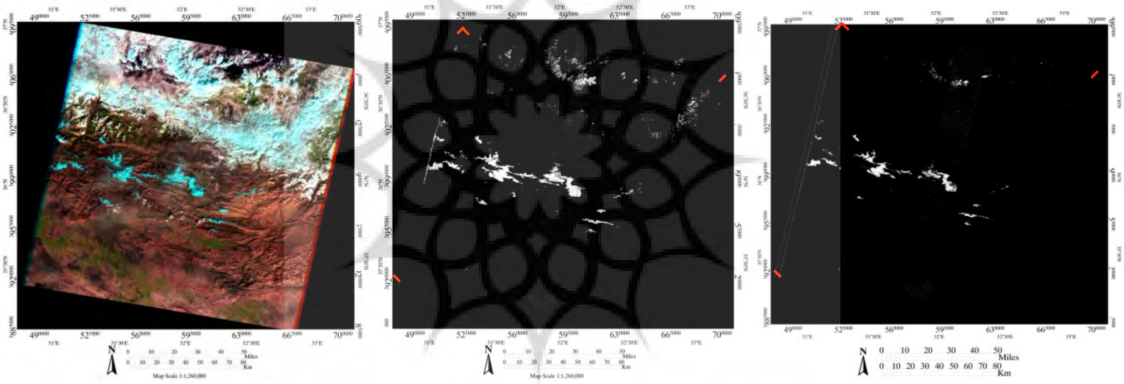

a B

Figure 10. a) Landsat Image (RGB:345), b) SCA derived from Eq 3, c) SCA derived from Eq 4

Figure 11 shows the SCA fraction in the sub-basins during 2006-2007 using ETM+ images; interpolated linearly for days that no images were available. The daily SCA fraction during the snowmelt season in 2007 for 6 HRU is derived and Snow depletion curve correction is applied with respect to the degree-day factor and daily temperature above the critical temperature in the melting season. Corrected depletions curves in 6 HRU using ETM+ images are shown in the Figure 12. It should be noted that differences between the SCA retrieved from MODIS snow product and Landsat images are due to calculating of maximum snow extent in MODIS snow product, which leads to an accuracy fall due to obtaining SCA in fewer time intervals.

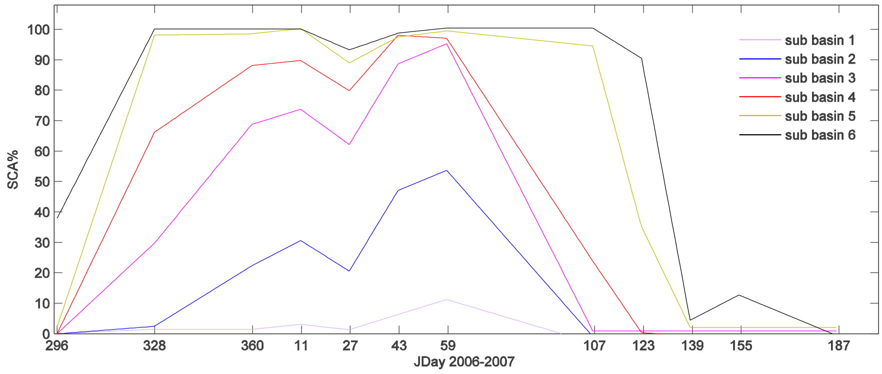

Figure 11. The SCA derived from Landsat ETM+ during 2006-2007

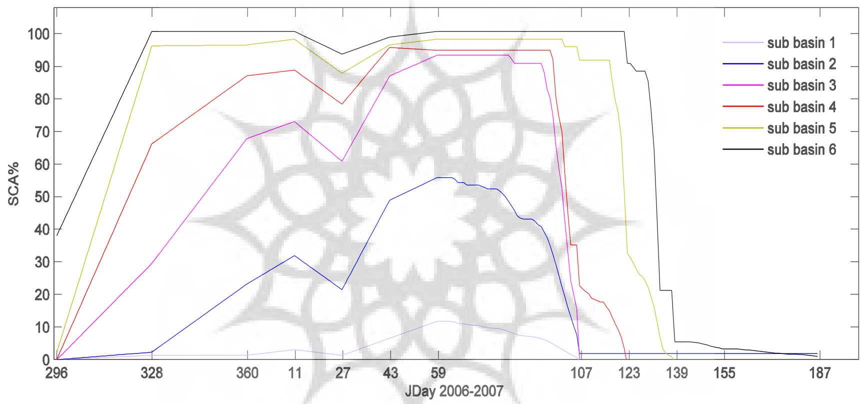

Figure 12. The corrected SCA Derived from Landsat ETM+ during 2006-2007

4.3. Snow Runoff Model (SRM)

The Snowmelt Runoff Model (SRM) developed by Martinec, Rango *et al.*, (1998) is used in this study for runoff modeling in our study basin. This model has been applied in more than 100 basins in 29 different countries around the world with various areas from 0.8 km2 to 917,444 km^2 (Martinec, Rango *et al*. 1998). SRM is a degree-day based deterministic hydrologic model that simulates daily snowmelt and rainfall runoff in mountainous basins. Required input variables for SRM includes daily temperature, precipitation and snow covered area. The daily runoff is computed using (Martinec, Rango *et al*. 1998):

$$Q_n = K_n Q_{n-1} + (1 - K_n)\frac{10000}{86400}\sum_i [C_{Si,n} a_{i,n}(T_{i,n} + \Delta T_{i,n})S_{i,n} + C_{Ri,n} P_{i,n}]A_i \quad \textbf{(14)}$$

In this equation, n is the day number; i is HRU index; k is the recession coefficient; C_S is the snowmelt runoff loss factor; C_R is the rainfall loss factor; $T+\Delta T$ is the air temperature above the threshold of melt including measured temperature in station plus temperature correction for mean elevation station minus critical temperature; P is the precipitation amount falling as rain or snow and A is the area.

The recession coefficient equals to the ratio of runoff on consecutive days when there is no added snowmelt and rain runoff. It can be computed from an archived runoff data as a function of Q, so that nonlinearity of the storage can be explained (Nagler, Rott *et al*. 2008). To derive k, archived basin's runoff in n_{th} day is plotted against $n+1_{th}$ day; it has been shown in Figure 13. Then slope and y intercept of the fitted line, calculated by weighted least squares method, are used in the equation (15) (Martinec *et al*., 1994).

$$K_{n+1} = aQ_{n^{-b}} \quad \textbf{(15)}$$

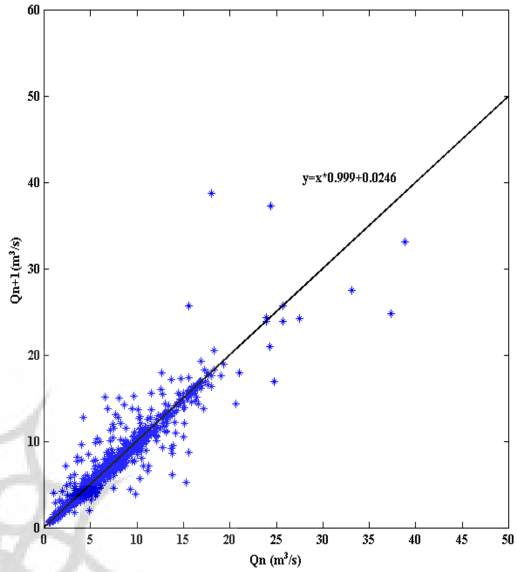

Figure 13. Stream Discharge $\mathbf{Q_n}$ against $\mathbf{Q_{n+1}}$ and Fitted Line

where, a is slope, b is y intercept and Q_n is n_{th} day runoff.

Interpolation methodology used for T and P distributed measurement and degree-day factor and runoff coefficients calculation were described in the section 3.2.1. Fraction of snow cover measurement explained in 3.2.2. Mean values of these variables and parameters for each HRU is then employed in the SRM (Martinec, Rango *et al*., 1998; Nagler, Rott *et al*., 2008).

5. Results and Discussion

SRM is performed for the water year 2006-2007. Model accuracy is explored by R^2, a measure of model efficiency and D_v according to equations (16) and (17), respectively (Martinec, Rango *et al*., 1998).

$$D_V = \frac{V_R - V_R'}{V_R} * 100 \quad \textbf{(16)}$$

$$R^2 = 1 - \frac{\sum_{i=1}^{n} (Q_i - Q_i')^2}{\sum_{i=1}^{n} (Q_i - \bar{Q})^2} \quad \textbf{(17)}$$

Figure 14 includes the measured and modeled runoff and accuracy parameters using corrected SCA driven from MODIS 8-Day product. Figure 15 includes measured and modeled runoff and accuracy parameters using corrected SCA driven from Landsat images.

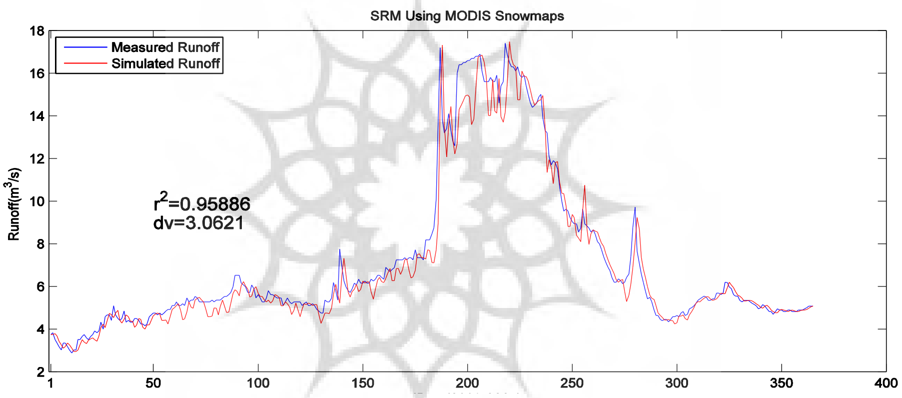

Figure 14. Daily SRM using MODIS snow Product (JDay starting from 2006-2007 water year)

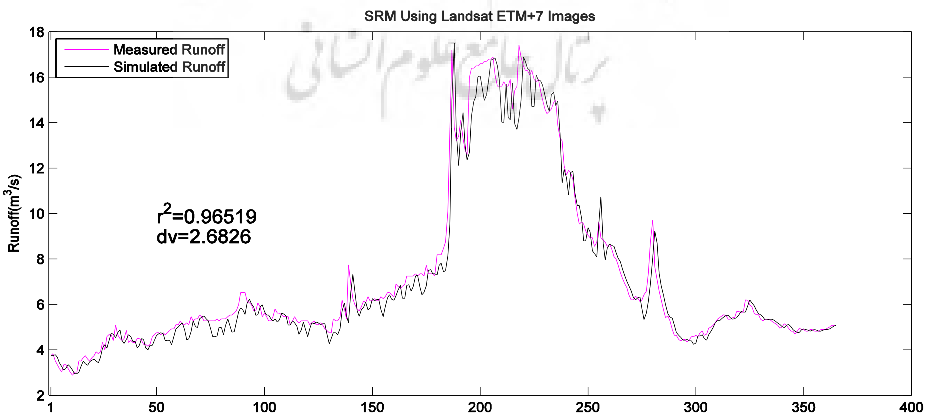

Figure 15. Daily SRM using landsat ETM+ images (JDay starting from 2006-2007 water year)

Differences between measured and modeled runoff are observed mainly before the snowmelt season, when the runoff is as a result of the rainfall and not the snowmelt water. Moreover, after a heavy rainfall modeling the response of basin needs more investigations.

Results show that this approach has the potential to be implemented in a prototype project for monitoring SCA and even forecasting snowmelt runoff in a web based interface system for the end users in this field of interest (it should be noted that forecasting needs data assimilation using climatologic data). For instance, snow runoff modeling can be useful in water management for both managers and users while irrigation schedule would be defined through the knowledge of estimated runoff at the end of season. Weekly and bi-weekly forecasts can be computed using the average temperature degree, precipitations and SCA during last ten years to adapt and calibrate SRM for a specific case study. SCA driven from MODIS product due to its application usage and also ease of access and process can be useful in this application.

6. Conclusion

In this study, SRM over a mountainous watershed in south of Ablorz Mountain and Hableh-Roud river basin has been implemented. Various data including meteorological data, geological maps and remotely sensed image data are processed to provide the inputs of SRM. Two different optical images were used in the snowmelt modeling for a SCA calculation to reach better accuracy in daily runoff modeling. Albeit, Landsat revisit time is 16 days and MODIS revisit time is 12 hours, SCA derived from Landsat images shows better agreement in measured runoff especially in melt season due to a better pixel resolution (30 meters versus 500 meters). However, SRM should be applied for several years to define whether using Landsat for snowmelt modeling will result in a more accurate modeling compared to MODIS snow maps. Due to free access to high level processed MODIS snow maps and also high temporal frequency compared to Landsat, using MODIS products in runoff modeling is more beneficiary in hydrological applications and is preferable compared to Landsat images.

One of the SRM's weaknesses is assuming a snowpack layer as a homogenous medium with uniform properties. Using field experiments to obtain more information during snowmelt season and modeling snowpack properties in addition to SCA could be helpful in daily SRM improvement. This information is also an important requirement in snowmelt forecast applications, when dynamic changes in snow grain size and density in different days of year (seasonal snowpack evolution) and from year to year affect estimations accuracy.

In addition, different satellite images and synoptic meteorological data using fusion and assimilation methods, respectively could be utilized to improve the model. For instance, fusion of visible images with SAR images and LST[1] products in decision level could be an effective approach in this criterion. SCA could also be improved using fractional snow cover estimation by unmixing methods. As SWE estimation is possible using microwave spectrum due to microwave penetration ability in snowpack layers, some more investigations should be also done for re-sampling methods on passive products for better integration with higher spatial resolution dataset to be utilized in such runoff models.

Acknowledgement

This work has been funded by Semnan Water Management Organization. We express our gratitude to Mr. Abyati, Khamoushi and Taheri for their helpful suggestions. We also thank NASA and UGSG for providing free Landsat and MODIS data.

References

[1] Baumgartner, M. F. and G. Apfl (1994), Monitoring snow cover variations in the Alps using the Alpine Snow Cover Analysis System (ASCAS). *Mountain environments in changing climates. Routledge, New York, New York, USA*, 108-120.

[2] Chander, Gyanesh, Brian L. Markham, and Dennis L. Helder. (2009), "Summary of current radiometric calibration coefficients for Landsat MSS, TM, ETM+, and EO-1 ALI sensors." *Remote Sensing of Environment* 113(5): 893-903.

[3] Cronshey, R., H.Mccuen, R., Miller, N., Rawls, W., Robims, S., & Woodward, D., (1986), *Urban Hydrology for Small Watersheds*.

[4] Dadashi khanghah, S. and A. A. Matkan (2007), *Snow cover detection using Image processing algorithms in Karaj and latian Basins* (In Persian). Faculty of Earth

1 Land Surface Temperature

Sciences. Tehran, Shahid Beheshti University. Msc.

[5] DeWalle, D. and A. Rango, (2008), *Principles of snow hydrology*, Cambridge University Press.

[6] Dobreva, I. D. and A. G. Klein, (2011), "Fractional snow cover mapping through artificial neural network analysis of MODIS surface reflectance." *Remote Sensing of Environment*.

[7] Elachi, C. and J. Van Zyl, (2006), *Introduction to the physics and techniques of remote sensing*, John Wiley and Sons.

[8] Hall, D. K., Riggs, G. A., Salomonson, V. V., Barton, J. S., Casey, K., Chien, J. Y. L., ... & Tait, A. B. (2001), "Algorithm theoretical basis document (ATBD) for the MODIS snow and sea ice-mapping algorithms." Sep.

[9] Irish, R., (2000), "Landsat 7 science data users handbook." *National Aeronautics and Space Administration*.

[10] Irish, R. R., Barker, J. L., Goward, S. N., & Arvidson, T. (2006), "Characterization of the Landsat-7 ETM Automated Cloud-Cover Assessment (ACCA) Algorithm." Photogrammetric Engineering & Remote Sensing 72(10): 1179-1188.

[11] Liang, S. (2008). Advances in Land Remote Sensing: System, Modelling, I*nversion and Application*, Springer.

[12] Martinec, J., Rango, A., & Roberts, R., (1994), Snowmelt runoff model (SRM) user’s manual. Retrieved from http://www.mastergardeners.nmsu.edu/pubs/research/water/SRMSpecRep100.pdf

[13] Martinec, J., Rango, A., Roberts, R., & Baumgartner, M. F. (1998), *Snowmelt runoff model (SRM) user's manual*, Geograph. Inst. d. Univ.

[14] Mountain environments in changing climates. Routledge, New York, New York, USA: 108–120.

[15] Michael, F. and A. R. Baumgartner, (1995), "A microcomputer-based alpine snow-cover analysis system (ASCAS)." *Photogrammetric engineering and remote sensing* 61(12): 1475-1486.

[16] Nagler, T., Rott, H., Malcher, P., & Müller, F. (2008), "Assimilation of meteorological and remote sensing data for snowmelt runoff forecasting." *Remote Sensing of Environment* 112(4): 1408-1420.

[17] Najafzadeh, R., Abrishamchi, A., Tajrishi, M., (2004), *Runoff simulation with snowmelt runoff modeling* (In Persian)."

[18] Rango, A., (1980), Operational Applications of Satellite Snow Cover Observations." *Jawra Journal of the American Water Resources Association* 16(6): 1066-1073.

[19] Riggs, G. and Hall, D., (2011), "MODIS Snow and Ice Products, and Their

Assessment and Applications." *Land Remote Sensing and Global Environmental Change*: 681-707.

[20] Riggs, G. A., Hall, D. K., & Salomonson, V. V. (2007), "MODIS Snow Products User Guide to Collection 5." Online article, retrieved on January 2.

[21] Solberg, R., Koren, H., Amlien, J., Malnes, E., Schuler, D. V., & Orthe, N. K. (2010), "The development of new algorithms for remote sensing of snow conditions based on data from the catchment of Øvre Heimdalsvatn and the vicinity." *Hydrobiologia* 642(1): 35-46.

[22] Vuyovich, C. and J. M. Jacobs (2011), "Snowpack and runoff generation using AMSR-E passive microwave observations in the Upper Helmand Watershed, Afghanistan." *Remote Sensing of Environment*.

[23] Zhang, C., Li, W., & Travis, D. (2007). "Gaps-fill of SLC-off Landsat ETM+ satellite image using a geostatistical approach." *International Journal of Remote Sensing* 28(22): 5103-5122.

[24] Zhang, Y., (2004). "Understanding image fusion." *Photogrammetric engineering and remote sensing* 70(6): 657-661.

مدلسازی رواناب حاصل از ذوب برف با استفاده از داده های هواشناسی، ژئولوژی و سنجش از دوری

نسترن صابری[۱]، سعید همایونی[۲]، مهدی معتق[۳]

[۱]دانشجوی دکتری، گروه جغرافیا، دانشگاه واترلو، کانادا
[۲] استادیار،گروه جغرافیا، دانشگاه اتاوا، کانادا
[۳] استادیار،گروه مهندسی نقشه برداری و ژئوماتیک، پردیس دانشکده های فنی، دانشگاه تهران

تاریخ دریافت: 90/12/15 **تاریخ پذیرش: 91/10/12**

جمع‌آوری و تحلیل اطلاعات جغرافیایی امکان پایش و مدیریت گستره منابع طبیعی را به صورت کارایی فراهم می‌آورد. به عنوان نمونه در مناطق خشک و نیمه خشک که مدیریت منابع آب از اهمیت بالایی برخوردار است، شناخت و مطالعه‌ی ذخایر برفي به عنوان تأمین‌کننده‌ی‌جریان پایه‌ي رودخانه‌ها و سرآغاز اصلي منابع آب شیرین در حوضه‌هاي برف‌گیر و مرتفع، نقش مهمی در برنامه‌ریزی و مدیریت مصرف منابع آب ایفا می‌کند. با استفاده از فن‌آوري سنجش از دور تهیه‌ي نقشه‌ي پوشش برف و محاسبه‌ی پارامترهاي برف در مقیاس بزرگ و با صرف هزینه‌ی کمتر نسبت به روش‌هاي زمیني ممکن شده‌است. با توجه به پارامترهای گسترده مورد نیاز در مدل‌های هیدرولوژیکی از جمله مدل رواناب ذوب برف SRM (Snowmelt Runoff Model) جمع‌آوری و همگن‌سازی این داده‌ها نیازمند دانش بالایی است. در این تحقیق با استفاده از تلفیق این اطلاعات شامل: اطلاعات هواشناسي، هیدرومتري ایستگاه‌ها، ویژگي‌هاي حوضه و اطلاعات جمع‌آوري شده از داده‌های مشاهداتی ماهواره‌اي، مقدار رواناب حاصل از ذوب برف را به صورت روزانه محاسبه مي‌شود. تغییرات سطح پوشش برف حوضه آبریز سیمین‌دشت واقع در فیروزکوه تهران با استفاده از محصول سطح پوشش برف روزانه با استفاده از سنجنده MODIS با قدرت تفکیک مکانی 500 متر (MOD10A2.5) در سال آبی 1386 1385 استخراج شد. به منظور مقایسه دقت برف‌سنجی با استفاده از تصاویر سنجنده +ETM ماهواره Landsat-7 با دقت مکانی 30 متر و دوره بازگشت زمانی 16 روز نیز تغییرات سطح برف محاسبه شد. با تأمین پارامترها و متغیرهای مورد نیاز مدل رواناب ذوب برف(SRM) با استفاده از اطلاعات هواشناسي و هیدرومتري ایستگاه‌ها، ویژگي هاي حوضه، پارامتر سطح پوشش برف و پارامتر رطوبت برف استخراج شده از تصاویر ماهواره‌ای، مقدار رواناب روزانه مدلسازی شد. دقت مدل با استفاده از محاسبه اختلاف حجم رواناب سالانه شبیه‌سازی و واقعی، و برآورد مجذور هم‌بستگی دبی روزانه شبیه‌سازی و واقعی محاسبه شد. ارزیابی نتایج مدلسازی حاکی از تطابق بالای رواناب مدلسازی و واقعی با استفاده از هر دو نوع تصویر و دقت بالاتر مدلسازی با استفاده از تصاویر Landsat است. هرچند دقت با استفاده از محصول پوشش برف MODIS پایین تر بود، ولی به دلیل تصویربرداری با دوره بازگشت کوتاه‌تر و حجم پایین‌تر پردازش با استفاده از این تصاویر، استفاده از این محصول توصیه می‌شود. توسعه مدل در پیش‌بینی رواناب با استفاده از تلفیق دیگر اندازه‌گیری‌ها و نیز مدل‌های فیزیکی می‌تواند زمینه تحقیقات آینده باشد.